Preprints.org

Review

Bioinspired Mechanical Materials —Development of High-Toughness Ceramics through Complexation of Calcium Phosphate and Organic Polymers

Tadashi Mizutani [*] and Kohei Okuda

Review

Bioinspired Mechanical Materials—Development of High-Toughness Ceramics through Complexation of Calcium Phosphate and Organic Polymers

Tadashi Mizutani * and Kohei Okuda

Department of Applied Chemistry, Faculty of Science and Engineering, Doshisha University; Kyotanabe, Kyoto 610-0394, Japan

Abstract: Inspired by the process of bone formation in living organisms, many studies have been conducted to develop organic-inorganic composite materials by generating calcium phosphate crystals within solutions or dispersions of polymers with appropriate functional groups. Bones are composite materials consisting of organic polymers (mainly Type I collagen), carbonated apatite, and water, with volume fractions 35-45%, 35-45%, 15-25%, respectively. Carbonated apatite in bone contributes to rigidity, while organic polymers and water contribute to toughness. The inorganic crystal, carbonated apatite, is a plate-shaped crystal with dimensions of 50 nm × 25 nm × 1-4 nm, generating a significant organic-inorganic interface due to its nanoscale size. This interface is believed to absorb externally applied forces to dissipate mechanical energy to thermal energy. Creating such nanometer-scale structures using top-down approaches is challenging, making bottom-up methods like co-precipitation of polymer and inorganic crystals more suitable. In this account, efforts to develop eco-friendly mechanical materials using biomass such as cellulose and starch based on the bottom-up approach to bone-like composites are described.

Keywords: Bioceramics; bone; composite; mechanical material; hydroxyapatite; polysaccharide; eco-friendly; water-resistance

1. Introduction

Plastics are extensively used as structural and mechanical materials in numerous products due to their excellent mechanical properties, lightweight nature, affordability, and good processability. Before the invention of plastics, materials like wood and bamboo were commonly used, but plastics have largely replaced them in many applications. However, there are several issues associated with the continued use of plastics. Firstly, plastics rely on fossil resources such as petroleum, leading to concerns about resource depletion and carbon dioxide emissions during incineration. Additionally, many plastics lack biodegradability, contributing to problems like marine pollution caused by microplastics, raising significant environmental concerns.[0] There is another concern on the use of plastics as structural materials because plastics generates poisonous gas when it burns. Potential alternatives to plastics include cellulose and biodegradable plastics. The mass production of parts of industrial products using bone and wood is challenging, because their anisotropic mechanical properties would make a molding process difficult.

On the other hand, aside from cellulose, materials such as bones, teeth, shells, horns, and crustacean shells have been used by living organisms as structural materials. These materials are composites of organic polymers and inorganic crystals.[2] The inorganic crystals are calcium phosphates or calcium carbonates, while the organic polymers are proteins and polysaccharides such as collagen and chitin. These composites form through the growth of inorganic crystals on the surface of organic polymers,[3] resulting in relatively lightweight and mechanically robust properties. If these materials can be industrially produced, they could serve as environmentally friendly alternatives to plastics.[4,5] We review here the structure and biosynthesis of bones, synthetic strategies of bioinspired organic-inorganic composites, and synthesis and mechanical properties of hydroxyapatite-polysaccharide composites.

2. The structure of bone and related tissues

Bone consists of three major components, carbonated apatite (nonometer sized calcium phosphate crystals), collagen-I fibers, and water in a volume ratio of approximately 56-60:30-40:10.[6,7,8] Carbonated apatite crystals have dimensions of 50 nm in length, 25 nm in width, and a thickness ranging from 1 nm to 4 nm.[9] The small crystal size of carbonated apatite is advantageous in terms of mechanical strength.[10] Based on the crystal size we can calculate the interface area between carbonated apatite and the organic phase being *ca.* 210 m²/g. The brick-and-mortar structure (Figure 1) formed by carbonated apatite crystals and collagen fibers contributed to toughness of bone.[Error! Bookmark not defined.,11,12,13,14] One of the major properties of bone is stiffness, which can support and protect a body from deformation. The elastic moduli of bone range from 2 to 33 GPa, and the bending strengths range from 27 to 308 MPa.[Error! Bookmark not defined.,15] Water plays an important role in the mechanical properties of bone: water removal caused increased stiffness but decreased toughness of bone.[16] Therefore, water contributes to toughness of bone. To understand the mechanical function of bone, it is necessary consider the interfaces and connections between bones and soft tissues. The elastic moduli of the soft tissues are 0.5-1 MPa (cartilage), 50-150 MPa (enthesis), and 0.45 GPa (tendon).[17] The stiffness of the soft tissues varies depending on the degree of mineralization.
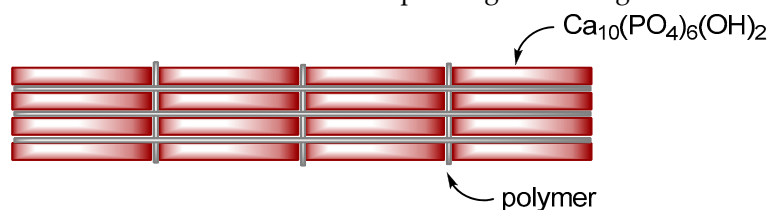

Figure 1. Brick-and-mortar structure of bone and polymer-HAP composites prevents fragile fracture.

2.1. Carbonated apatite and its interface

Hydroxyapatite (HAP) has a molecular formula of $Ca_{10}(PO_4)_6(OH)_2$. The crystals of HAP are hexagonal with *a* 9.417 Å and *c* 6.875 Å.[18] HAP is the most stable phase formed when calcium ions and phosphate ions are reacted under alkaline conditions. It is well known that isomorphous substitution occurs frequently: calcium ion is substituted by Sr, Ba, Mg, Mn, K, Na, Fe, and phosphate ion by AsO_4^{3-}, CO_3^{2-} and VO_4^{3-}.[19] Carbonated apatite (CAP) is formed by substitution of OH^- or PO_4^{3-} of hydroxyapatite by carbonate ions, CO_3^{2-}. We refer to hydroxyapatite in which the OH group has been replaced by carbonate ions as Type A carbonated apatite, and the PO_4^{3-} replaced by carbonate ions as Type B carbonated apatite.[20] The most common crystal morphology is needle-like, and it grows along the *c*-axis direction. It is known that citric acid is adsorbed on the side surfaces of needle-shaped crystals of carbonated apatite of bone.[21] There is ongoing debate regarding the presence of organic materials on the surface of CAP, and NMR studies have revealed the binding of polysaccharides to the surface.[22] NMR studies also proved that the surface of mature bone mineral particles is the hydrated amorphous calcium phosphate. The HPO_4^{2-} ions are concentrated at the surface of bone mineral particles in the amorphous surface layer whose thickness was estimated to be about 0.8 nm for a 4-nm thick particle carbonated apatite.[23]

2.2. Biosynthesis of bone

Bone is formed by precipitation of amorphous calcium phosphate on collagen fibers, and its subsequent crystallization. Acidic proteins containing many phosphate and/or carboxylate groups in the side chain play an important role in biomineralization.[Error! Bookmark not defined.,Error! Bookmark not defined.,24,] These anionic groups can concentrate calcium ions, and reaction with phosphate ions to precipitate amorphous calcium phosphate. Hierarchical structures of bone are described in several reviews.[Error! Bookmark not defined.,Error! Bookmark not defined.,25,26,27]

2.3. Bioceramics and woods as mechanical materials

Bone and woods are lightweight, ductile, and biodegradable.[28,29] Although bone and woods are superior materials, there is disadvantage of them if we use them as an industrial material. It is difficult to form the desired shape due to their anisotropic properties, and they are not suitable for mass production, that is, molding process is inefficient.

3. Composite materials related to bone

3.1. General features of organic-inorganic composites

Organic-inorganic composite materials can be broadly classified into two categories, ceramics-reinforced plastics and polymer-reinforced ceramics. The former is achieved by enhancing the low rigidity of the organic phase through the addition of the inorganic phase. Glass fiber-reinforced plastics, clay-polyamide composites[30] and automobile tire are commonly used in daily life. If plastics is too soft to resist external stress, we can add inorganic fillers such as glass fibers to increase stiffness of plastics. The major component of the composites of this category is an organic phase, and the minor component is an inorganic phase. "Polymer-reinforced ceramics" is to improve the brittleness of ceramics by incorporating organic polymers, as seen in laminated glass. For laminated glass, due to a sandwiched structure of glass plate - polymer film - glass plate, it would not be broken into pieces if a shock is given owing to the organic polymer film. The major component of this category is an inorganic phase, and the minor component is an organic phase. Bone is polymer-reinforced ceramics, and can be roughly described as nanometer sized laminated glass with a brick-and-mortar structure (Figure 1).

Table 1. Classification of organic-inorganic composites.

	Ceramic reinforced polymer	Polymer reinforced ceramics
Major component	Polymer (matrix)	Ceramics (filler)
Minor component	Ceramics (filler)	Polymers (matrix)
Examples	Glass-fiber reinforced plastics	Laminated glass
	Polyamide-clay composites	Bones
	Tire	Teeth

3.2. Preparation of organic-inorganic composites

For the preparation of organic-inorganic composites, following three protocols have been reported:
1. Direct mixinig of polymer and inorganic crystals
2. Polymerization of monomer in the presence of inorganic crystal powder
3. Crystallization of inorganic phase in the presence of organic polymer

As the first protocol example, Bonfield and coworkers reported that a composite of polyethylene and apatite was created by mixing both components.[31] The elastic modulus of the composite is linearly related to the volume fraction of apatite, and when the volume fraction was varied from 0 to 0.6, the elastic modulus ranged from 1 to 12 GPa. The second protocol was employed to prepare the composite of poly(L-lactic acid-co-glycolic acid) and hydroxyapatite.[32] Polyamide-clay composites are prepared by ring-open polymerization of ε-caprolactam in the presence of clay mineral, montmorillonite, which has been ion-exchanged by ω-carboxyalkylammonium. Thus, the composite is also prepared in the second protocol.[Error! Bookmark not defined.] The third protocol is biomimetic, bottom-up approach, and suitable for preparation of nanometer-sized inorganic crystals which are bound to the polymer phase. Stupp et al. reported that precipitation occurs when an aqueous solution of polyglutamic acid was mixed with calcium hydroxide and phosphoric acid, and the resulting precipitate is the composite of the polymer and apatite.[33] Polyglutamic acid sodium salt, polylysine hydrochloride, and polyacrylic acid 1 mM aqueous solution was mixed with calcium hydroxide and phosphoric acid, and pH of the mixture was adjusted to 7.4 at 37 °C. The composites are called

organoapatite, and X-ray diffraction showed that the composites contained poorly crystalline hydroxyapatite. The ratio of Ca/P was close to 1.6, the theoretical value of hydroxyapatite in the absence of polymer, while the ratio was 1.4 to 1.6 in the presence of the polymers, showing that calcium-deficient hydroxyapatite formed.

Anionic functional groups like those found in proteins play a crucial role in the biomineralization of biomaterials such as bone.[34,35,36,37,38,39,40,41,42,43,44,45,46,47] Akkus and coworkers crystallized HAP in the presence of charged peptides, and performed a systematic investigation on the effects of charged peptides on the HAP morphology.[48] They found that anionic peptides such as poly-L-Asp and poly-L-Glu bind to HAP than cationic peptides such as poly-L-Lys and polu-L-Arg. Negatively charged peptides lead to smaller crystals of HAP than positively charged ones. Research involving the complexation of hydroxyapatite with various polymers and polymer gels has been carried out and reviewed.[Error! Bookmark not defined.,49,50,51,52,53,54,55,56,57,58,59,60,61,62,63,64,65,,66,67, ,68,69,70,71] Carbonated apatite in bone is a hexagonal crystal, and citrate anions adsorb onto the *a* and *b* faces.[Error! Bookmark not defined.] Anionic functional groups adsorb onto the *a* and *b* faces of hydroxyapatite, while cations adsorb onto the *c* face.[Error! Bookmark not defined.,72] Thus, by adding calcium ions and phosphate ions to solutions of polymers with anionic functional groups like carboxylate or phosphate ions under an alkaline condition, the polymers adsorb onto the *a* and *b* faces of apatite through their anions, leading to the growth of crystals along the *c*-axis. As a result, it might be possible to control the crystal size in the nanometer range and achieve the composite formation of organic polymer chains and needle-like or plate-like inorganic crystals bonded with each other with aligned orientations (Figure 1). Formation of the brick-and-mortar structure is crucial for toughness of the composites.[Error! Bookmark not defined.,Error! Bookmark not defined.,Error! Bookmark not defined.,Error! Bookmark not defined.] The polymers used here can include petroleum-derived synthetic polymers, proteins, and polysaccharides, but using biomass-derived polysaccharides synthesized from carbon dioxide through photosynthesis could address carbon dioxide emission and environmental issues.

3.3. Composite of hydroxyapatite and polysaccharide

Use of polysaccharides as an organic component of the composite is an attractive strategy because the biomass is carbon neutral and degraded biologically. There have been several studies on the preparation of the composites of hydroxyapatite and polysaccharides.[Error! Bookmark not defined.,Error! Bookmark not defined.,73,74,75] Yao and coworkers crystallized HAP in the presence of polysaccharides and found that the crystal size of HAP decreased in the order, amylose (-OH) > chitosan (-NH$_2$, -NHCOCH$_3$, -OH) > carrageenan (-OSO$_3^-$, -OH) > pectin (-COO$^-$, -OH).[Error! Bookmark not defined.] The polar functional groups of these polysaccharides are shown in the parenthesis. Therefore, polysaccharides have an ability to regulate crystallization of HAP. It seems that –COO$^-$ group is the most effective in suppressing crystal growth of HAP. We can avoid environmental issues such as microplastics pollution of sea water by employing polysaccharide-based mechanical materials. Annual production of cellulose is 1×10^{11} ton, while that of starch is 4×10^7 ton, use of cellulose as an organic phase of the composite seems attractive. Yu and coworkers reported a composite of cellulose nanofibers and TiO$_2$-coated mica. It showed a bending strength of 281 MPa and elastic modulus of 20 GPa.[Error! Bookmark not defined.]

3.3.1. Creating Structural Materials with Environmentally Friendly Materials and Processes

By adding calcium ions and phosphate ions to a solution or dispersion of polysaccharides, it's possible to simultaneously synthesize hydroxyapatite crystals and perform organic-inorganic complexation. In this process, the characteristics of the composites change based on factors such as the temperature during co-precipitation, the concentration of polymers and inorganic ions, and the types of counter ions. The process can be carried out in water between room temperature and 90°C, with optimal results often achieved around 50-70°C. Conducting complexation at lower temperatures leads to slow crystal growth of hydroxyapatite and the formation of materials with characteristics closer to amorphous, resulting in lower mechanical properties. On the other hand, complexation at higher temperatures like 90°C tends to lead to the dissociation of bonds between organic polymers
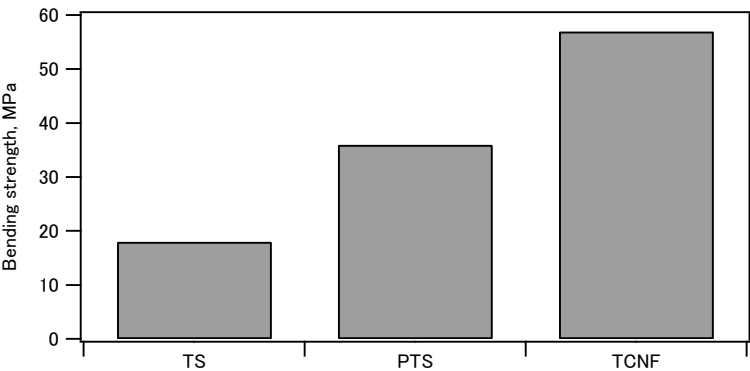
and inorganic crystal surfaces, leading to a decrease in mechanical properties.[Error! Bookmark not defined.] Sodium or ammonium can be used as counter cations for phosphate ions, and the choice of counter cations also affects complexation. For instance, the complex with the highest elasticity was obtained when ammonium was used as the counter cation for carboxymethyl cellulose (CMC) complexation. The obtained precipitate can be separated through methods like filtration, then after drying, molded into shapes using uniaxial pressure molding. The molding conditions range from room temperature to 120°C, and the pressure is approximately 120-300 MPa. The molded forms created in this manner, upon conducting bending tests, exhibited flexural strengths of 50-110 MPa and flexural moduli of around 5-10 GPa. In comparison to general plastics, the flexural strength was similar, while the flexural modulus exceeded that of plastics (Table 2).[Error! Bookmark not defined.]

Table 2. Comparison of mechanical properties of the polysaccharide-HAP composites with those of plastics[76].

	Bending strength, MPa	Elastic modulus, GPa	Density, g/cm³	Uniaxial press pressure, MPa
PTS-HAP, HAP 70 wt%	47	4.9	1.72	120
CMC-HAP, HAP 70 wt%	113	7.7	1.8	120
TCNF-HAP, HAP 62 wt%	80	11.6	1.94	300
Poly(methyl methacrylate)	118	3.4	1.19	
Polyamide-6	118	2.8	1.14	

3.3.2. Starch-hydroxyapatite composites

Starch is, among polysaccharides, a widely distributed biopolymer produced by many plants consisting of a mixture of amylose, which is composed of glucose units polymerized in a linear fashion, and amylopectin, which has a branched structure. Some naturally occurring starches have hydroxy groups partially esterified with phosphate. Additionally, starches with phosphate esterification, containing more phosphate groups, are synthesized and used for industrial purposes. When starch is heated with water, it undergoes gelation (gelatinization) and disperses in water. We gelatinized tapioca starch with and without phosphate esterification (containing 0.013% phosphorus by weight) and conducted co-precipitation by adding calcium ions and phosphate ions. The resulting white precipitate was molded into shapes using uniaxial pressure molding, and the mechanical strength was evaluated through three-point bending tests.[Error! Bookmark not defined.] The bending strength, elastic modulus, and strain at failure of the molded compacts of phosphorylated tapioca starch (PTS)/regular tapioca starch (TS) and HAP are shown in Figure 2. It was found that phosphorylated starch showed superior mechanical properties compared to regular starch. This was ascribed to the contribution of the phosphate groups to crystal nucleation and binding at the organic-inorganic interface.
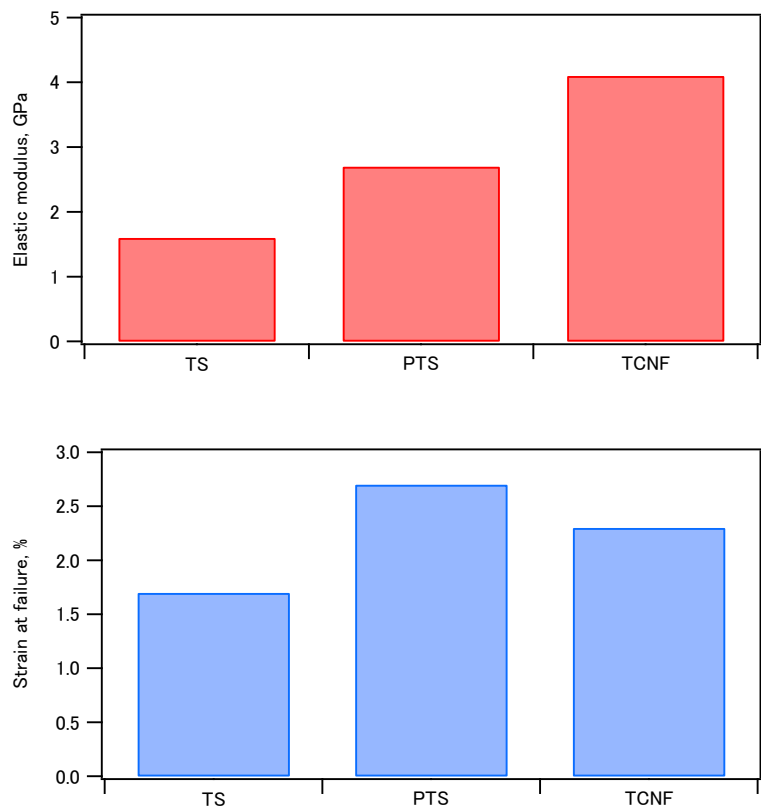
Figure 2. Comparison of bending strength, elastic modulus and strain at failure evaluated by three-point bending test of tapioca starch (TS)-hydroxyapatite, phosphorylated tapioca starch (PTS)-hydroxyapaite, and TEMPO-oxidized cellulose nanofibers (TCNF)-hydroxyapatite composites containing 70 wt% of hydroxyapatite.**Error! Bookmark not defined.,Error! Bookmark not defined..**

Figure 3 shows the plot of elastic modulus of the PTS-HAP composite compacts against the volume fraction of HAP in the composites. The elastic moduli linearly increased with increasing the HAP volume fractions, indicating that HAP contributes stiffness of the composites. On the other hand, non-phosphorylated starch-HAP composites did not show meaningful correlation between elastic moduli and the volume fraction of HAP.
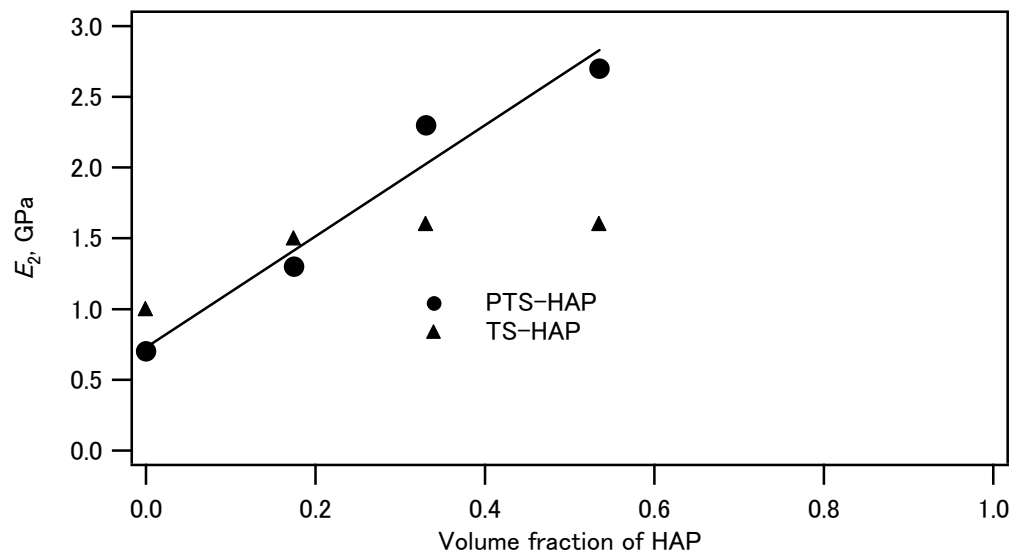

Figure 3. Plot of elastic moduli of phosphorylated tapioca starch (PTS)-HAP composites and tapioca starch (TS)-HAP composites against the volume fraction of HAP.

3.3.3. Cellulose nanofibers-hydroxyapatite composites

TEMPO-oxidized cellulose nanofibers (TCNF) are obtained by oxidizing the C-6 carbon carrying a primary hydroxyl group on the surface of nanofibers into a carboxyl group. The cross-section of nanofibers consists of 6 × 6 glucose units, with every other glucose on the surface oxidized to glucuronic acid (Figure 4).[77] The width is around 3-4 nm, and the length is several micrometers. Carboxylate groups on the surface of nanofibers can bind with calcium ions, and it is expected that if hydroxyapatite crystal nucleation occurs, hydroxyapatite crystals will grow around TCNF fibers, aligning the *c*-axis of hydroxyapatite parallel to form a brick-and-mortar structure. By dropping phosphate ions and calcium ions into TCNF dispersion, we obtained co-precipitates and molded this white powder into shapes using uniaxial pressure molding. The mechanical properties of the compacts were evaluated by three-point bending tests. The compacts exhibited higher bending strength and elastic moduli than those of the compacts of phosphorylated starch-hydroxyapatite composites (Figure 2). It is noteworthy that the fracture surface was not flat, implying non-brittle fracture (Figure 5). Fiber-like structures of lengths approximately 140 ± 30 mm were observed. The compacts of the TCNF-HAP composites bent and did not break into two pieces during bending tests. This fracture surface is similar to that of the lamellar bone of a tibia of a rat.[78]
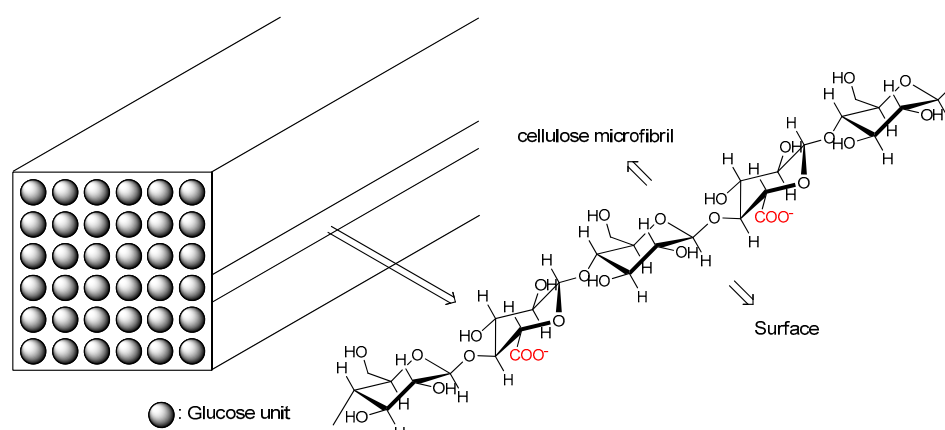

Figure 4. Schematic representation of TEMPO-oxidized cellulose nanofibers.**Error! Bookmark not defined..**
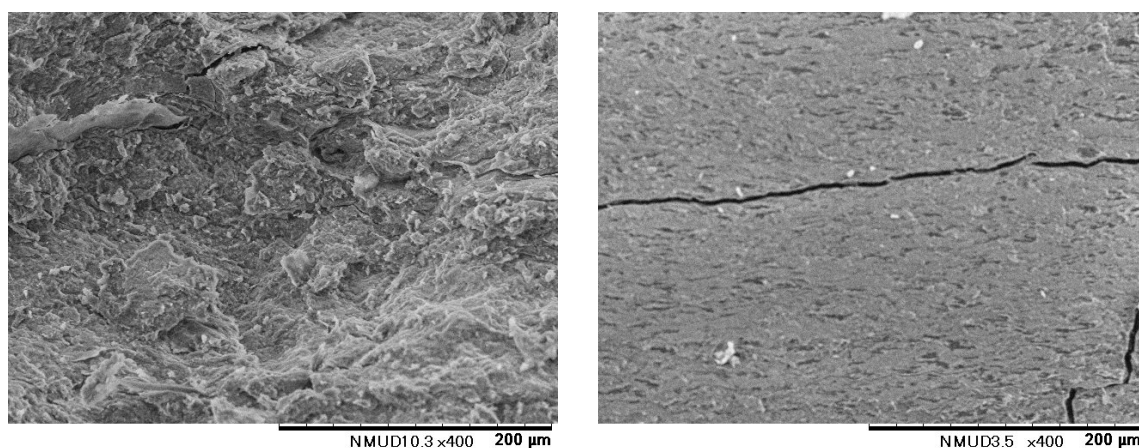

Figure 5. Fracture surface of the compact of the TCNF-HAP composite coprecipitated at 90 °C (left) and that of the compact of the phosphorylated starch-HAP composite coprecipitated at 70 °C (right). In the three point bending test of the TCNF-HAP compacts, the compacts only bent so the fracture surface was produced by pulling the compact by bare hands.

The fracture mode of the compacts of the TCNF-HAP composites was found to depend on the polymer aggregation state during coprecipitation. It was observed that the formation of a fiber structure by polymers within the composite hinders crack propagation and suppresses brittle fracture

under stress.[79] During bending tests, the molded specimens only bent and did not separate into two parts. For instance, when creating a composite of hydroxyapatite with polymers like starch or carboxymethyl cellulose, the resulting composite exhibited brittle fracture.[80,81] Conversely, materials composed of cellulose nano-fibers, which adopt a fibrous structure due to cellulose nanofibers aggregation, did not exhibit brittle fracture when subjected to stress. Furthermore, it was discovered that this fracture pattern varied depending on the concentration of TCNF during co-precipitation. When coprecipitation was performed using a low concentration of TCNF, the formed material exhibited brittle fracture and separated into two pieces. Under dilute conditions, homogeneous nucleation of HAP is more likely to occur, making it less likely to form a brick-and-mortar structure. Figure 6 schematically illustrates coprecipitation of TCNF-HAP composites at a low concentration and an intermediate concentration of TCNF. At an intermediate concentration of TCNF, heterogeneous nucleation of HAP is the major process, while at a low concentration of TCNF, both homogeneous and heterogeneous nucleation could occur to prevent formation of the brick-and-mortar structure.
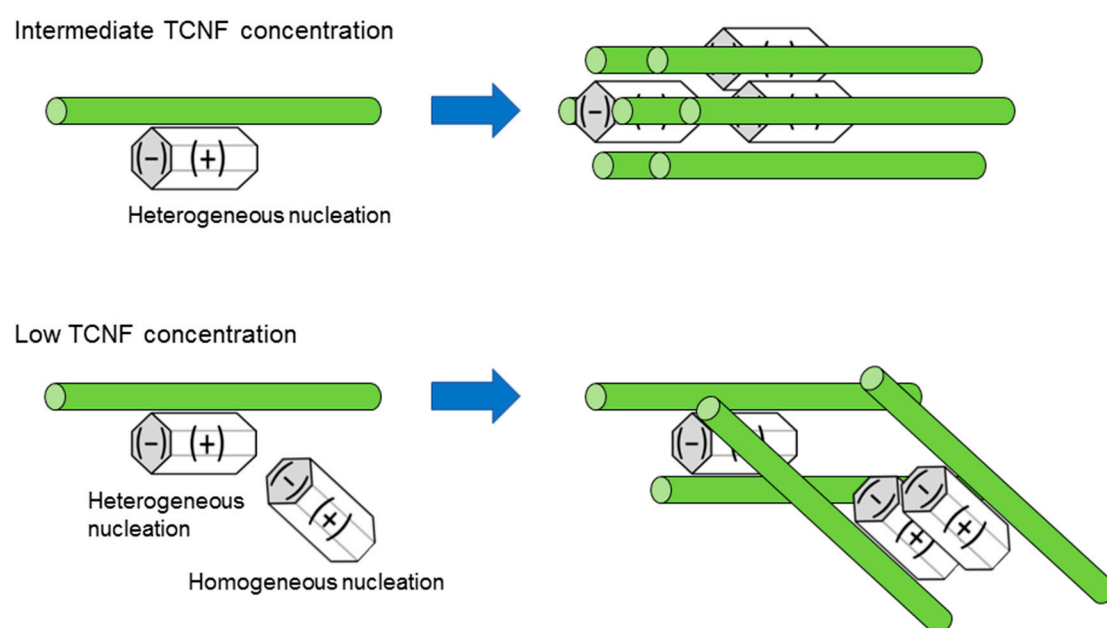

Figure 6. Schematic representation of coprecipitation of TCNF and HAP. At an intermediate concentration of TCNF, heterogeneous nucleation of HAP on TCNF is the major pathway to produce an aligned composite. At a low concentration of TCNF both heterogeneous and homogeneous nucleation occur to prevent formation of the fibrous structure.

Through this approach, the composites formed by polymers and nano-fibers with hydroxyapatite demonstrated mechanical properties such as flexural strength and flexural modulus that were comparable to plastics (Table 2). Particularly, the flexural modulus exceeded that of plastics, indicating greater rigidity. However, these composites are not water resistant. When immersed in water, the molded compacts easily disintegrated, resulting in a loss of structural material functionality. To address this issue, we investigated how the partial acylation of hydroxyl groups in polysaccharides would impact mechanical properties and water resistance.[82,83]

3.4. Introduction of hydrophobic groups for water resistance enhancement

The surfaces of polysaccharides and hydroxyapatite are hydrophilic and readily hydrated. Thus, when molded composites are immersed in water, they often undergo substantial swelling, resulting in significant changes in mechanical properties. In bone's apatite, the carboxyl groups of citric acid adsorb to calcium ions through ionic bonding on the *a* and *b* faces. Accordingly, the methylene groups of citric acid face outward, contributing to the hydrophobicity of apatite crystals. Bone contains

around 10% water, and when dried, it becomes more elastic but also more brittle, compromising toughness.**Error! Bookmark not defined.** This implies that water content plays a significant role in bone's mechanical properties, especially toughness. The synthesized composites of cellulose or starch and hydroxyapatite demonstrated significant water absorption, leading to a near-complete loss of mechanical strength. Therefore, the introduction of acyl groups to hydroxyl groups, which are abundant in polysaccharides, was considered as a means to improve the water resistance of the composites.

3.4.1. Acylation of phosphorylated starch-HAP composites

The composite of starch-hydroxyapatite was dispersed in polar solvents such as dimethyl sulfoxide or *N,N*-dimethylformamide and heated at 60-120°C for 4-8 hours after adding vinyl carboxylate such as vinyl acetate, vinyl hexanoylate, vinyl laurate and vinyl benzoate, and potassium carbonate (Figure 7). The progress of acylation was confirmed from the infrared absorption spectra. The absorbance at 1750 cm^{-1} for aliphatic acyl groups and 1728 cm^{-1} for an aromatic acyl group increased, indicating that acylation of the hydroxy groups of the starch proceeded. The water absorption rates were evaluated by immersing the molded compacts before and after acylation in water for 24 hours at room temperature, as shown in Figure 8. The water absorption rate before acylation was 136%, and acylation significantly reduced the water absorption rate. Particularly, benzoyl and lauroyl groups were effective in reducing water absorption. Furthermore, when comparing the flexural strength before and after water immersion (Figure 9), the acetylated compact exhibited 17% of that of the dry compact, the benzoic ester showed 52% of that of the dry compact, and the lauric ester demonstrated 66% of that of the dry compact. Except for the acetylated composite, acylation significantly improved water resistance, especially for the lauric ester.

Furthermore, acylation of the starch-hydroxyapatite composite significantly influenced its mechanical and thermal properties. The stress-strain curves of PTS-HAP composite and its acylated ones are shown in Figure 10. The stress-strain curves clearly demonstrate that the composite compacts were softer by acylation, particularly by the long acyl group. Comparison of Figures 10 and 11 shows that the composite compacts become even more flexible when soaked in water. The flexural strength, the elastic modulus, and the strain at failure of the composite before acylation were 47.3 MPa, 4.9 GPa, and 1.8%, respectively. After benzoylation, they became 28.7 MPa, 2.7 GPa, and 1.7%, and after lauroylation, they became 9.0 MPa, 0.2 GPa, and 5.8%. Particularly, lauroylation resulted in decreased rigidity and increased flexibility. Additionally, the lauroylated composite demonstrated fluidity at 120°C, indicating thermoplastic behavior. The density of the molded form of the lauroylated composite was 1.2 g/cm³, demonstrating a lightweight characteristic similar to plastics.
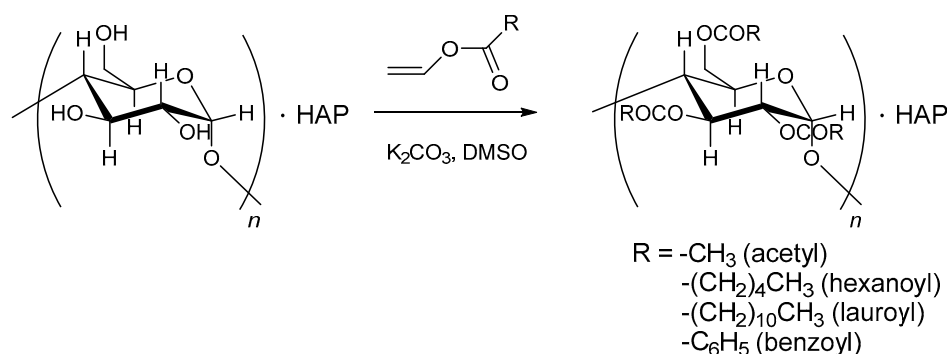

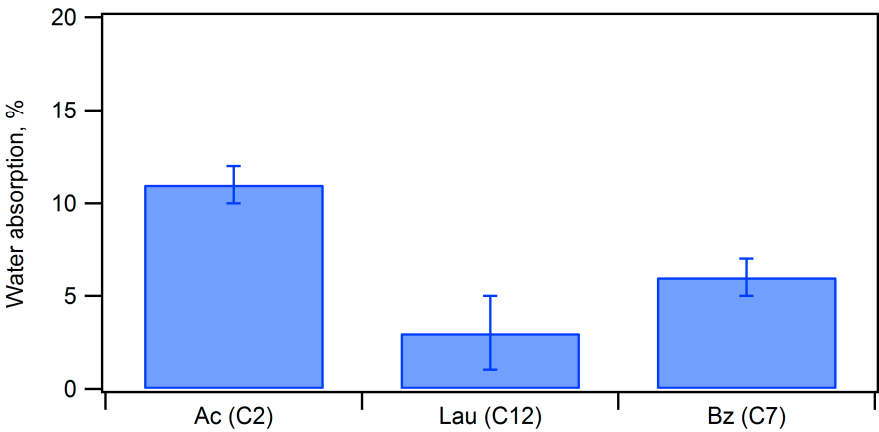**Figure 7.** Acylation of the composites of starch and hydroxyapatite.

Figure 8. Water absorption of the compacts of PTS-HAP composites containing 66 wt% HAP acylated with acetyl (Ac), lauroyl (Lau) and benzoyl (Bz) groups.
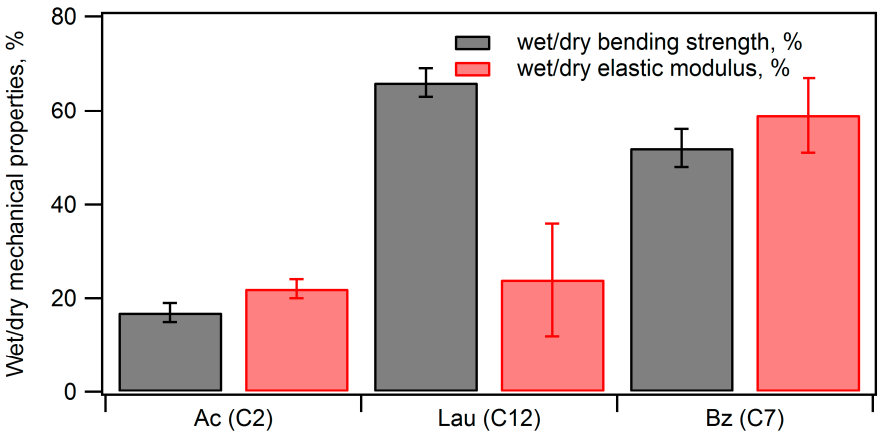

Figure 9. The ratios of bending strength and elastic modulus after water immersion to those before water immersion of the acylated PTS-HAP composite compacts.
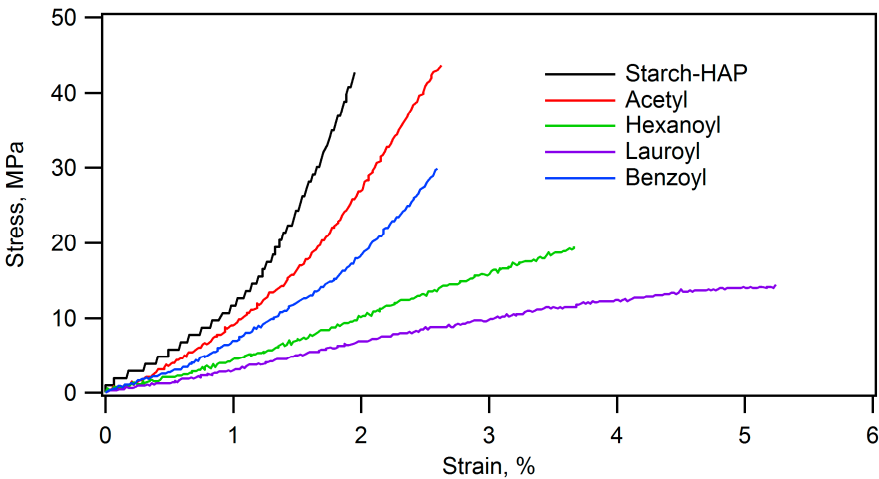

Figure 10. Stress-strain curves of the phosphorylated starch-HAP composite containing 50 wt% of the inorganic phase and its acylated composites.
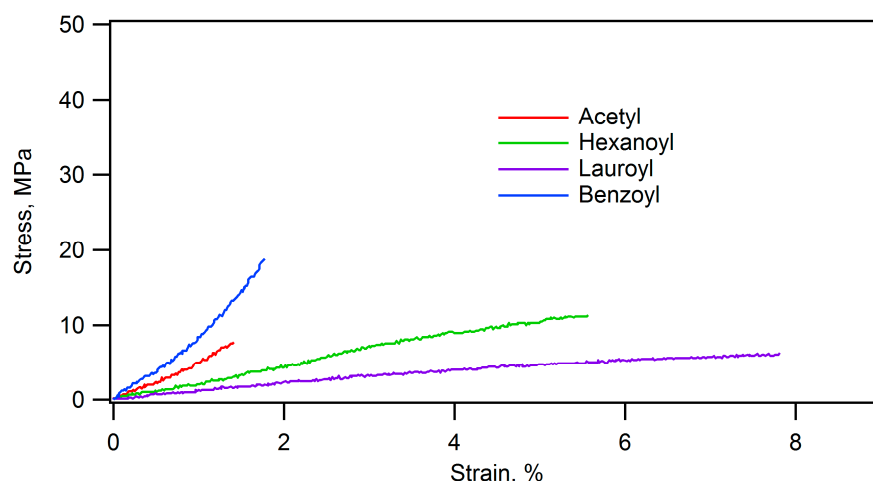
Figure 11. Stress-strain curves of the acylated composites of phosphorylated starch-HAP after immersion in water at 25 °C for 24 h.

3.4.2. Acylation of TCNF-HAP composites

As described above, the TCNF-HAP composites showed a unique fracture mode similar to curdboard. The compacts also adsorbed much water when immersed in water, and its stiffness was lost in water. Because TCNF has a lot of carboxylate groups, the composites are hydrophilic. If the composites can be made hydrophobic with the non-brittle property unchanged, the composites can be used in many applications. We acylated the TCNF-HAP composites containing 62 wt% HAP in a similar fashion as that used for acylation of the starch-HAP composites. The obtained composites were uniaxially pressed in a mold to prepare the compacts for bending test. Water absorption of the acylated compacts, immersed in water at 25 °C for 24 h, are shown in Figure 12. The acetylated composite adsorbed 88% water but hexanoylated one adsorbed only 11%. The water absorption increased as the alkyl chain length increased further. The mechanical properties after immersed in water are shown in Figure 13. The acetylated composite showed almost no stiffness after immersed in water, while hexanoylated and oxtanoylated ones showed *ca.* 30 % of bending strength and *ca.* 20 % of elastic modulus of the pristine compacts.
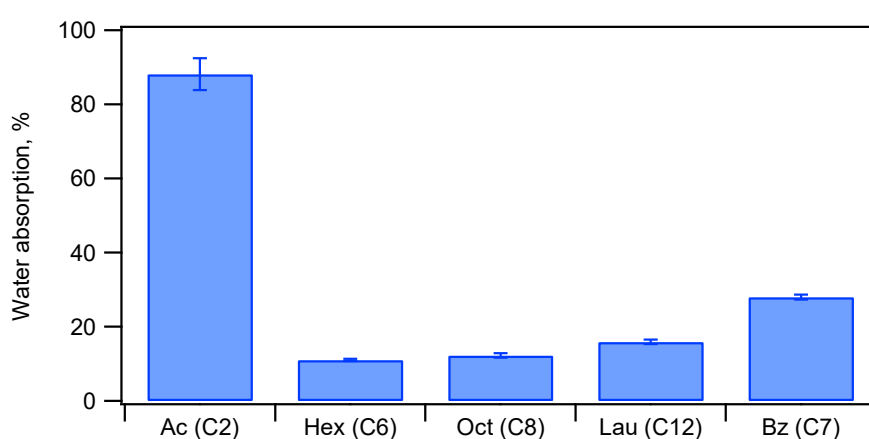

Figure 12. Water absorption of the compacts of TCNF-HAP composites containing 62 wt% HAP acylated with acetyl (Ac), hexanoyl (Hex), octanoyl (Oct), lauroyl (Lau) and benzoyl (Bz) groups.
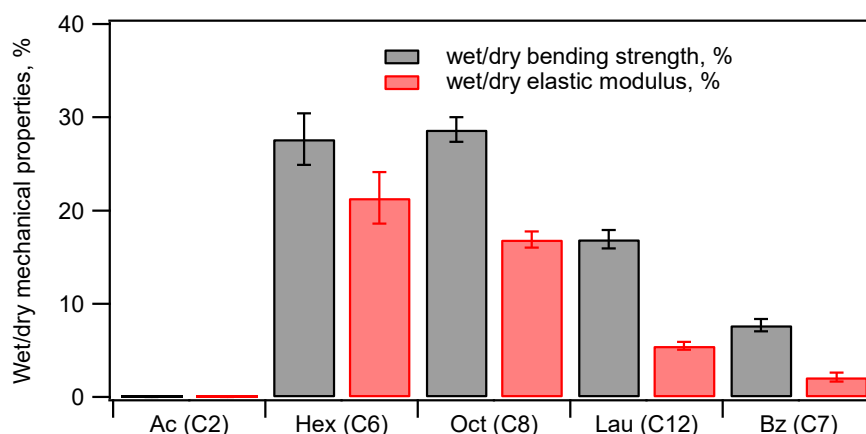
Figure 13. The ratios of bending strength and elastic modulus after water immersion to those before water immersion of the acylated TCNF-HAP composite compacts.

3.4.3. Comparison of water resistance of starch-HAP, cellulose-HAP, and poly(DL-lactide)-HAP

While both starch and cellulose are polysaccharides composed of repeating glucose units, their mechanical properties differ when complexed with hydroxyapatite. Figure 5 displays fracture surfaces from bending tests of molded compacts where TEMPO-oxidized cellulose nanofibers and phosphorylated tapioca starch were complexed with hydroxyapatite at 70°C. In the case of starch, cracks propagate linearly leading to brittle fracture, whereas for cellulose nanofibers, a fibrous structure is observed. This indicates that the fibrous structure of cellulose nanofibers improves brittleness. The composite of cellulose nanofibers and hydroxyapatite does not separate into two fragments even during bending tests, which is why the fracture surface after manually tearing is shown.

Ritchie and coworkers reported that the composite of poly(DL-lactide) and HAP exhibits the bending strength of 23 MPa, while it decreased to 3 MPa when the compact was left at 37 °C for 30 h in a humid environment. The ratio of the wet bending strength to the dry one is 13% for the composite. Compared with the ratio, the ratio of lauroylated PTS-HAP was 66% and that of octanoylated TCNF-HAP was 30%. The number of anionic groups decreases in the order, TCNF > PTS > poly(DL-lactide). The comparison suggest that hydrophobicity of the polymer is not the dominant factor determining water resistance of the composite, but there is optimum hydrophilicity/hydrophobicity balance of the polymer to endow the composite with water resistance (see Figure 14).
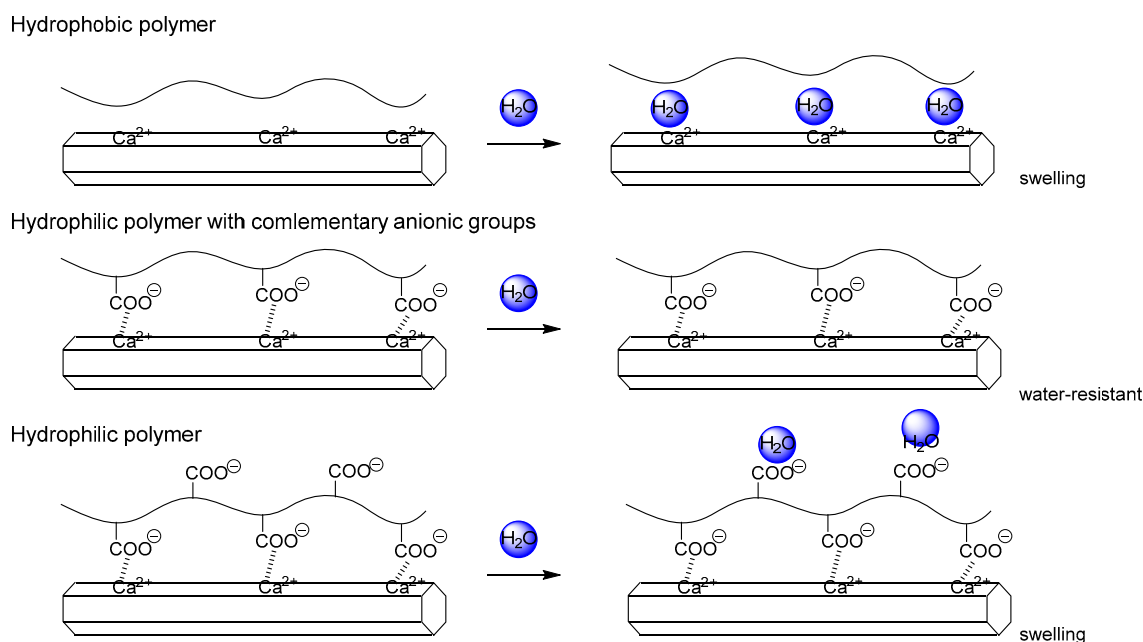
Figure 14. Schematic representation of water resistance of the composites of hydroxyapatite and hydrophilic and hydrophobic polymers.

4. Future Outlook

The co-precipitation complexation, where calcium ions and phosphate ions are added to polymer solutions or dispersions, allowing the growth of calcium phosphate crystals using polymers as scaffolds, is an excellent method to uniformly composite nanometer-sized crystals under mild conditions via a simple process. In the case of hydroxyapatite, employing polymers with anionic functional groups leads to efficient co-precipitation, where the attractive interaction between the polymer and the surface of the HAP crystals are expected to result in good mechanical properties. On the other hand, polymers with polar groups and hydroxyapatite tend to readily hydrate in water, leading to swelling and significant changes in mechanical properties of the molded compacts in the presence of water. To enhance the water resistance of the composites, a balance between polar and nonpolar groups is essential, and acylation reactions of the hydroxy groups of polysaccharide proves effective. Furthermore, the formation of fibrous structures through polymer aggregation can prevent brittle fracture in the composites, leading to more reliable structural materials. In particular, the use of polymers derived from cellulose makes it easier to induce such fibrous structures. Additionally, since cellulose is a type of biomass, it holds promise as an environmentally friendly structural material candidate in the future. In this account, we describe development of the polymer-hydroxyapatite composites and their mechanical and water-resistant properties, focusing on a coprecipitation process. Recent investigations indicate that mixing of inorganic crystals with a large aspect ratio and homogeneous size, which are prepared in advance, with polymers lead to composites with excellent stiffness and strength, comparable to those of bone and teeth.**Error! Bookmark not defined.**,[84,85] Therefore, synthesis of inorganic crystals with a large aspect ratio can be crucial for development of bioinspired mechanical materials. Although coprecipitation is a simple process under ambient conditions, it may be necessary to fine-tune the heterogeneous crystallization in the presence of polymer.

Conflicts of Interest: The authors declare no conflict of interest..

References

1.　Eerkes-Medrano, D.; Thompson, R. C.; Aldridge, D. C. Microplastics in freshwater systems: A review of the emerging threats, identification of knowledge gaps and prioritisation of research needs. *Water Research (Oxford)* **2015**, *75*, 63-82. DOI:10.1016/j.watres.2015.02.012.

2. Stock, S. R. The Mineral-Collagen Interface in Bone. *Calcif. Tissue Int.* **2015**, *97*, 262-280.

3. Nudelman, F.; Lausch, A. J.; Sommerdijk, N. A. J. M.; Sone, E. D. In vitro models of collagen biomineralization. *J. Struct. Biol.* **2013**, *183*, 258-269. DOI:10.1016/j.jsb.2013.04.003.

4. Guan, Q.; Yang, H.; Han, Z.; Ling, Z.; Yu, S. An all-natural bioinspired structural material for plastic replacement. *Nature communications* **2020**, *11*, 5401 DOI:10.1038/s41467-020-19174-1.

5. Curto, M.; Le Gall, M.; Catarino, A. I.; Niu, Z.; Davies, P.; Everaert, G.; Dhakal, H. N. Long-term durability and ecotoxicity of biocomposites in marine environments: a review. *RSC Adv.* **2021**, *11*, 32917-32941 DOI:10.1039/d1ra03023j.

6. Olszta, M. J.; Cheng, X.; Jee, S. S.; Kumar, R.; Kim, Y.; Kaufman, M. J.; Douglas, E. P.; Gower, L. B. Bone structure and formation: A new perspective. *Mater. Sci. Eng., R* **2007**, *R58*, 77-116.

7. Granke, M.; Does, M. D.; Nyman, J. S. The Role of Water Compartments in the Material Properties of Cortical Bone. *Calcif. Tissue Int.* **2015**, *97*, 292-307.

8. Dorozhkin, S. V.; Epple, M. Biological and Medical Significance of Calcium Phosphates. *Angew. Chem. Int. Ed.* **2002**, *41*, 3130-3146.

9. Weiner, S.; Wagner, H. D. THE MATERIAL BONE: Structure-Mechanical Function Relations. *Annu. Rev. Mater. Sci.* **1998**, *28*, 271-298.

10. Gao, H.; Ji, B.; Jager, I. L.; Arzt, E.; Fratzl, P. Materials become insensitive to flaws at nanoscale: Lessons from nature. *Proc. Nat. Acad. Sci. USA* **2003**, *100*, 5597-5600.

11. Bouville, F.; Maire, E.; Meille, S.; Van de Moortele, B.; Stevenson, A. J.; Deville, S. Strong, tough and stiff bioinspired ceramics from brittle constituents. *Nature Mater.* **2014**, *13*, 508-514.

12. Wilbrink, D. V.; Utz, M.; Ritchie, R. O.; Begley, M. R. Scaling of strength and ductility in bioinspired brick and mortar composites. *Appl. Phys. Lett.* **2010**, *97*, No. 193701

13. Wang, R.; Gupta, H. S. Deformation and Fracture Mechanisms of Bone and Nacre. *Annu. Rev. Mater. Res.* **2011**, *41*, 41–73.

14. Sakhavand, N.; Shahsavari, R. Universal composition-structure property maps for natural and biomimetic platelet-matrix composites and stacked heterostructures. *Nat. Commun.* **2015**, *6*, 6523.

15. Currey, J. D. What determines the bending strength of compact bone? *J. Exp. Biol.* **1999**, 202, 2495-2503.

16. Nyman, J. S.; Roy, A.; Shen, X.; Acuna, R. L.; Tyler, J. H.; Wang, X. The influence of water removal on the strength and toughness of cortical bone. *J. Biomech.* **2006**, *39*, 931-938.

17. Pitta Kruize, C.; Panahkhahi, S.; Putra, N. E.; Diaz-Payno, P.; van Osch, G.; Zadpoor, A. A.; Mirzaali, M. J. Biomimetic Approaches for the Design and Fabrication of Bone-to-Soft Tissue Interfaces. *ACS Biomater. Sci. Eng.* **2023**, *9*, 3810-3831.

18. Hughes, J. M.; Cameron, M.; Crowley, K. D. Structural variations in natural F, OH, and Cl apatites. *Am. Mineral.* **1989**, *74*, 870-876.

19. Dorozhkin, S. V. Calcium Orthophosphates in Nature, Biology and Medicine. *Materials* **2009**, *2*, 399-498.

20. Sato, K.; Kogure, T.; Kumagai, Y.; Tanaka, J. Crystal Orientation of Hydroxyapatite Induced by Ordered Carboxyl Groups. *J.Colloid Interface Sci.* **2001**, *240*, 133-138.

21. Hu, Y. -Y.; Rawal, A.; Schmidt-Rohr, K. Strongly bound citrate stabilizes the apatite nanocrystals in bone. *Proc. Natl. Acad. Sci. USA* **2010**, *52*, 22425-22429.

22. Wise, E. R.; Maltsev, S.; Davies, M. E.; Duer, M. J.; Jaeger, C.; Loveridge, N.; Murray, R. C.; Reid, D. G. The Organic-Mineral Interface in Bone Is Predominantly Polysaccharide. *Chem. Mater.* **2007**, *19*, 5055-5057.

23. Eden, M. Structure and formation of amorphous calcium phosphate and its role as surface layer of nanocrystalline apatite: Implications for bone mineralization. *Materialia* **2021**, *17*, 101107. DOI:10.1016/j.mtla.2021.101107.

24. George, A.; Veis, A. Phosphorylated Proteins and Control over Apatite Nucleation, Crystal Growth, and Inhibition. *Chem. Rev.* **2008**, *108*, 4670-4693.

25. Rho, J.; Kuhn-Spearing, L.; Zioupos, P. Mechanical properties and the hierarchical structure of bone. *Med. Eng. Phys.* **1998**, *20*, 92-102.

26. Barthelat, F.; Yin, Z.; Buehler, M. J. Structure and mechanics of interfaces in biological materials. *Nat. Rev. Mater.* **2016**, *1*, No. 16007.

27. Fratzl, P.; Weinkamer, R. Nature₅ hierarchical materials. *Prog. Mater. Sci.*, *52*, 1263-1334.

28. Espinosa, H. D.; Rim, J. E.; Barthelat, F.; Buehler, M. J. Merger of structure and material in nacre and bone? Perspectives on de novo biomimetic materials. *Prog. Mater. Sci.* **2009**, *54*, 1059–1100.

29.   Wagermaier, W.; Klaushofer, K.; Fratzl, P. Fragility of Bone Material Controlled by Internal Interfaces. *Calcif. Tissue Int.* **2015**, *97*, 201−212.

30.   Okada, A.; Usuki, A. Twenty Years of Polymer-Clay Nanocomposites. *Macromol. Mater. Eng.* **2006**, *291*, 1449-1476. DOI:10.1002/mame.200600260.

31.   Bonfield, W.; Grynpas, M. D.; Tully, A. E.; Bowman, J.; Abram, J. Hydroxyapatite reinforced polyethylene - a mechanically compatible implant material for bone replacement. *Biomaterials* **1981**, *2*, 185-186.

32.   Takeoka, Y.; Hayashi, M.; Sugiyama, N.; Yoshizawa-Fujita, M.; Aizawa, M.; Rikukawa, M. In situ preparation of poly(L-lactic acid-co-glycolic acid)/hydroxyapatite composites as artificial bone materials. *Polym. J. (Tokyo, Jpn.)* **2015**, *47*, 164-170.

33.   Stupp, S. I.; Ciegler, G. W. Organoapatite: Materials for artificial bone. I. Synthesis and microstructure. *J. Biomed. Mater. Res.* **1992**, *26*, 169-183.

34.   Embery, G.; Rees, S.; Hall, R.; Rose, K.; Waddington, R.; Shellis, P. Calcium- and hydroxyapatite binding properties of glucuronic acid-rich and iduronic acid-rich glycosaminoglycans and proteoglycans. *Eur. J. Oral Sci.* **1998**, *106*, 267−273.

35.   Kirkham, J.; Brookes, S. J.; Shore, R. C.; Wood, S. R.; Smith, D. A.; Zhang, J.; Chen, H.; Robinson, C. Physico-chemical properties of crystal surfaces in matrix-mineral interactions during mammalian biomineralisation. *Current Opin. Colloid Interface Sci.* **2002**, *7*, 124-132.

36.   Bertoni, E.; Bigi, A.; Falini, G.; Panzavolta, S. Roveri, N. Hydroxyapatite/polyacrylic acid nanocrystals, *J. Mater. Chem.*, **1999**, *9*, 779–782.

37.   Song, J.; Saiz, E.; Bertozzi, C. R. A New Approach to Mineralization of Biocompatible Hydrogel Scaffolds: An Efficient Process toward 3-Dimensional Bonelike Composites. *J. Am. Chem. Soc.* **2003**, *125*, 1236−1243.

38.   Kikuchi, M.; Ikoma, T.; Itoh, S.; Matsumoto, H. N.; Koyama, Y.; Takakuda, K.; Shinomiya, K.; Tanaka, J. Biomimetic synthesis of bone-like nanocomposites using the self-organization mechanism of hydroxyapatite and collagen. *Compos. Sci. Technol.* **2004**, *64*, 819−825.

39.   Pramanik, N.; Biswas, S. K.; Pramanik, P. Synthesis and Characterization of Hydroxyapatite/Poly(Vinyl Alcohol Phosphate) Nanocomposite Biomaterials, *Int. J. Appl. Ceram. Technol.*, **2008**, *5*, 20–28.

40.   Meldrum, F. C.; Coelfen, H. Controlling Mineral Morphologies and Structures in Biological and Synthetic Systems. *Chem. Rev.* **2008**, *108*, 4332−4432.

41.   Fujisawa, R.; Tamura, M. Acidic bone matrix proteins and their roles in calcification. *Front. Biosci.* **2012**, *17*, 1891−1903.

42.   Coleman, R. J.; Jack, K. S.; Perrier, S.; Grondahl, L. Hydroxyapatite Mineralization in the Presence of Anionic Polymers. *Cryst. Growth Des.* **2013**, *13*, 4252−4259.

43.   Veis, A.; Dorvee, J. R. Biomineralization Mechanisms: A New Paradigm for Crystal Nucleation in Organic Matrices. *Calcif. Tissue Int.* **2013**, *93*, 307−315.

44.   Zhou, Y.; Liu, Q.; Zhao, Z.; Wang, W.; Zheng, L.; Li, Z. Preparation and Characterization of Phosphorylated Collagen and Hydroxyapatite Composite as a Potential Bone Substitute, *Chem. Lett.*, **2013**, *42*, 83–85.

45.   Morimune-Moriya, S.; Kondo, S.; Sugawara-Narutaki, A.; Nishimura, T.; Kato, T.; Ohtsuki, C. Hydroxyapatite formation on oxidized cellulose nanofibers in a solution mimicking body fluid. *Polym. J.* **2015**, *47*, 158−163.

46.   Fang, W.; Zhang, H.; Yin, J.; Yang, B.; Zhang, Y.; Li, J.; Yao, F. Hydroxyapatite Crystal Formation in the Presence of Polysaccharide, *Cryst. Growth Des.*, **2016**, *16*, 1247–1255.

47.   Kusakabe, A.; Hirota, K.; Mizutani, T. Crystallisation of hydroxyapatite in phosphorylated poly(vinyl alcohol) as a synthetic route to tough mechanical hybrid materials, *Mater. Sci. Eng., C*, **2017**, *70*, 487–493.

48.   Diegmueller, J. J.; Cheng, X.; Akkus, O. Modulation of Hydroxyapatite Nanocrystal Size and Shape by Polyelectrolytic Peptides. *Cryst. Growth Desig.* **2009**, *9*, 5220-5226. DOI:10.1021/cg900750z.

49.   Mayer, G. Rigid Biological Systems as Models for Synthetic Composites. *Science* **2005**, *310*, 1144−1147.

50.   Schweizer, S.; Taubert, A. Polymer-Controlled, Bio-Inspired Calcium Phosphate Mineralization from Aqueous Solution. *Macromol. Biosci.* **2007**, *7*, 1085-1099.

51.   Palmer, L. C.; Newcomb, C. J.; Kaltz, S. R.; Spoerke, E. D.; Stupp, S. I. Biomimetic Systems for Hydroxyapatite Mineralization Inspired By Bone and Enamel. *Chem. Rev.* **2008**, *108*, 4754−4783.

52.   Munch, E.; Launey, M. E.; Alsem, D. H.; Saiz, E.; Tomsia, A. P.; Ritchie, R. O. Tough, Bio-Inspired Hybrid Materials. *Science* **2008**, *322*, 1516−1520.

53.   Roeder, R. K.; Converse, G. L.; Kane, R. J.; Yue, W. Hydroxyapatite-Reinforced Polymer Biocomposites for Synthetic Bone Substitutes. *JOM* **2008**, *60*, 38−45.

54. Li, B.; Wang, X.; Ma, J.; Huang, L. Preparation of phosphorylated chitosan/chitosan/hydroxyapatite composites by co-precipitation method. *Adv. Mater. Res.* **2009**, *79-82*, 401-404.

55. Nudelman, F.; Sommerdijk, N. A. J. M. Biomineralization as an inspiration for materials chemistry. *Angew. Chem., Int. Ed.* **2012**, *51*, 6582–6596.

56. Zhang, C.Y.; Chen, J.; Zhuang, Z.; Zhang, T.; Wang, X.P.; Fang, Q.F. In situ hybridization and characterization of fibrous hydroxyapatite/chitosan nanocomposite, *J. Appl. Polym. Sci.* **2012**, *124*, 397–402.

57. Onoki, T.; Nakahira, A.; Tago, T.; Hasegawa, Y.; Kuno, T. Novel low temperature processing techniques for apatite ceramics and chitosan polymer composite bulk materials and its mechanical properties. *Applied Surface Science* **2012**, *262*, 263-266.

58. Yang, L.; Ning, X.; Bai, Y.; Jia, W. A scalable synthesis of non-agglomerated and low-aspect ratio hydroxyapatite nanocrystals using gelatinized starch matrix. *Mater. Lett.* **2013**, *113*, 142-145.

59. Bleek, K.; Taubert, A. New developments in polymer controlled, bioinspired calcium phosphate mineralization from aqueous solution. *Acta Biomater.* **2013**, *9*, 6283–6321.

60. Ma, J.; Wang, J.; Ai, X.; Zhang, S. Biomimetic self-assembly of apatite hybrid materials: From a single molecular template to bi-/ multi-molecular templates. *Biotechnol. Adv.* **2014**, *32*, 744–760.

61. Won, J. -E.; El-Fiqi, A.; Jegal, S. -H.; Han, C. -M.; Lee, E. -J.; Knowles, J. C.; Kim, H. -W. Gelatin-apatite bone mimetic co-precipitates incorporated within biopolymer matrix to improve mechanical and biological properties useful for hard tissue repair. *J. Biomater. Appl.* **2014**, *28*, 1213-1225.

62. Li, J.; Baker, B. A.; Mou, X.; Ren, N.; Qiu, J.; Boughton, R. I.; Liu, H. Biopolymer/Calcium Phosphate Scaffolds for Bone Tissue Engineering. *Adv. Healthcare Mater.* **2014**, *3*, 469–484.

63. Shu, Y.; Yin, P.; Liang, B.; Wang, H.; Guo, L. Bioinspired Design and Assembly of Layered Double Hydroxide/Poly(vinyl alcohol) Film with High Mechanical Performance. *ACS Appl. Mater. Interfaces* **2014**, *6*, 15154–15161.

64. Cheng, Q.; Jiang, L.; Tang, Z. Bioinspired Layered Materials with Superior Mechanical Performance. *Acc. Chem. Res.* **2014**, *47*, 1256–1266.

65. Wegst, U. G. K.; Bai, H.; Saiz, E.; Tomsia, A. P.; Ritchie, R. O. Bioinspired structural materials. *Nat. Mater.* **2015**, *14*, 23–36.

66. Le, H.; Natesan, K.; Pranti-Haran, S. Mechanical property and biocompatibility of co-precipitated nano hydroxyapatite.gelatine composites. *J. Adv. Ceram.*, **2015**, *4*, 237-243.

67. Shakir, M.; Jolly, R.; Khan, M. S.; Iram, N. e.; Khan, H. M. Nano-hydroxyapatite/chitosan starch nanocomposite as a novel bone construct: Synthesis and in vitro studies. *Int. J. Biol. Macromol.* **2015**, *80*, 282-292.

68. Zakharov, N. A.; Demina, L. I.; Aliev, A. D.; Kiselev, M. R.; Matveev, V. V.; Orlov, M. A.; Zakharova, T. V.; Kuznetsov, N. T. Synthesis and Properties of Calcium Hydroxyapatite/Silk Fibroin Organomineral Composites. *Inorg. Mater.* **2017**, *53*, 333-342.

69. Miculescu, F.; Maidaniuc, A.; Voicu, S. I.; Thakur, V. K.; Stan, G. E.; Ciocan, L. T. Progress in Hydroxyapatite. Starch Based Sustainable Biomaterials for Biomedical Bone Substitution Applications. *ACS Sustainable Chem. Eng.* **2017**, *5*, 8491–8512.

70. Yang, R. L.; Zhu, Y. J.; Chen, F. F.; Qin, D. D.; Xiong, Z. C. Bioinspired Macroscopic Ribbon Fibers with a Nacre-Mimetic Architecture Based on Highly Ordered Alignment of Ultralong Hydroxyapatite Nanowires. *ACS Nano* **2018**, *12*, 12284–12295.

71. Zima, A. Hydroxyapatite-chitosan based bioactive hybrid biomaterials with improved mechanical strength. *Spectrochim. Acta A* **2018**, *193*, 175-184.

72. Kawasaki, T.; Takahashi, S.; Ikeda, K. Hydroxyapatite high-performance liquid chromatography: column performance for proteins. *Eur. J. Biochem.* **1985**, *152*, 361-371.

73. Kim, M.; Yeo, M.; Kim, M.; Kim, G. Biomimetic cellulose/calcium-deficient hydroxyapatite composite scaffolds fabricated using an electric field for bone tissue engineering. *RSC Adv.* **2018**, *8*, 20637–20647.

74. Malkaj, P.; Pierri, E.; Dalas, E. The crystallization of hydroxyapatite in the presence of sodium alginate. *J. Mater. Sci.: Mater. Med.* **2005**, *16*, 733–737.

75. Ingole, V. H.; Vuherer, T.; Maver, U.; Vinchurkar, A.; Ghule, A. V.; Kokol, V. Mechanical Properties and Cytotoxicity of Differently Structured Nanocellulose-hydroxyapatite Based Composites for Bone Regeneration Application. *Nanomaterials* **2020**, *10*, No. 25.

76. *Polymer Handbook*, 4th ed.; Brandrup, J.; Immergut, E. H.; Grulke, E. A., Eds.; John Wiley & Sons, Inc.: New York, 1999.

77. Okita, Y.; Saito, T.; Isogai, A. Entire Surface Oxidation of Various Cellulose Microfibrils by TEMPO-Mediated Oxidation. *Biomacromolecules* **2010**, *11*, 1696-1700. DOI:10.1021/bm100214b.

78. Weiner, S.; Addadi, L. Design strategies in mineralized biological materials. *J. Mater. Chem.* **1997**, *7*, 689–702.

79. Okuda, K.; Mizutani, T.; Hirota, K.; Hayashi, T.; Zinno, K. Nonbrittle Nanocomposite Materials Prepared by Coprecipitation of TEMPO-Oxidized Cellulose Nanofibers and Hydroxyapatite. *ACS Sustainable Chem. Eng.* **2021**, *9*, 158-167.

80. Okuda, K.; Hirota, K.; Mizutani, T.; Aoyama, Y. Co-precipitation of tapioca starch and hydroxyapatite. Effects of phosphorylation of starch on mechanical properties of the composites. *Results in Materials* **2019**, *3*, 100035.

81. Okuda, K.; Shigemasa, R.; Hirota, K.; Mizutani, T. In Situ Crystallization of Hydroxyapatite on Carboxymethyl Cellulose as a Biomimetic Approach to Biomass-Derived Composite Materials. *ACS Omega* **2022**, *7*, 12127-12137.

82. Okuda, K.; Aoyama, Y.; Hirota, K.; Mizutani, T. Effects of Hydration on Mechanical Properties of Acylated Hydroxyapatite-Starch Composites. *ACS Appl. Polym. Mater.* **2022**, *4*, 1666-1674.

83. Okuda, K.; Kido, E.; Hirota, K.; Mizutani, T. Water-resistant Tough Composites of Cellulose Nanofibers and Hydroxyapatite. *ACS Appl. Polym. Mater.* **2023**, *5*, in press. DOI:10.1021/acsapm.3c01292.

84. Das, P.; Malho, J.; Rahimi, K.; Schacher, F. H.; Wang, B.; Demco, D. E.; Walther, A. Nacre-mimetics with synthetic nanoclays up to ultrahigh aspect ratios. *Nature Commun.* **2015**, *6*, 5967. DOI:10.1038/ncomms6967.

85. Yu, H. -C.; Zhu, Y. -J.; Xiong, Z. -C.; Lu, B. -Q. Bioinspired fiberboard-and-mortar structural nanocomposite based on ultralong hydroxyapatite nanowires with high mechanical performance. *Chem. Eng. J.* **2020**, *399*, 125666.